

A virtual environment for ultrasound examination learning

Amel Ourahmoune, Chafiaa Hamitouche & Slimane Larabi

To cite this article: Amel Ourahmoune, Chafiaa Hamitouche & Slimane Larabi (2018): A virtual environment for ultrasound examination learning, Computer Methods in Biomechanics and Biomedical Engineering: Imaging & Visualization, DOI: [10.1080/21681163.2018.1505553](https://doi.org/10.1080/21681163.2018.1505553)

To link to this article: <https://doi.org/10.1080/21681163.2018.1505553>



Published online: 21 Aug 2018.



Submit your article to this journal [↗](#)



Article views: 9



View Crossmark data [↗](#)



A virtual environment for ultrasound examination learning

Amel Ourahmoune^{a,b}, Chafiaa Hamitouche^b and Slimane Larabi^a

^aDepartment of Computer Science, University of Science and Technology Houari Boumediene, Algiers, Algeria; ^bLaboratoire de Traitement de l'Information Medicale (LaTIM), IMT Atlantique, France

ABSTRACT

In this study, we propose a virtual learning environment for ultrasonography gestures based on an ultrasound (US) learning database. The learning database is comprised of US probe position and orientation, US images and force applied on the skin for each image. The intermediate images were inferred using the set of two-dimensional (2D) US images acquired at various force levels by the mean of interpolation method. A force feedback joystick with three degrees of freedom is used to monitor the applied forces. The proposed virtual environment was able to overcome the lack of immersion of the learner in the existing systems, especially, the US image deformation and force feedback feeling. In addition to the low cost, our system simulates, accurately, the US exam ensuring a good immersion to the learner with all senses involved in the US exam. An intelligent agent supervises the learner through the whole process. The virtual environment was evaluated by experts and trainees, and the results are presented and discussed.

ARTICLE HISTORY

Received 5 July 2017
Accepted 23 July 2018

KEYWORDS

Learning; virtual environment; simulation; haptic device; ultrasound probe; ultrasound

1. Introduction

Multiple imaging modalities exist for the evaluation or examination of anatomical structures; each one is suitable for specific structure, diagnosis and/or pathology. Ultrasound (US) imaging has been widely used as it is a non-ionising technique and constitutes as a first choice for many anatomical structures. However, performing an US examination involves a good hand–eye coordination and an ability to integrate the acquired information over time and space; the physician has to be able to imagine three-dimensional (3D) anatomy from 2D images and perform a diagnosis from this information. This makes the interpretation of US exam difficult, operator dependent and subjective due to the specular and diffused appearance of US image, leading to misdiagnosis. Thus, learning US image acquisition and diagnosis in the presence of an expert US radiologist becomes a necessary step for the beginner.

Current US examination training still follows the classical two-stage model:

- (i) Theoretical knowledge garnered using the major textbooks in the field,
- (ii) Practical knowledge achieved by performing US examination multiple times as possible, which implies a long learning curve.

This training method requires availability of patients and teachers. Reliability and quality of training also depends on the availability of pathologies examined. Kohn et al. (2004) reported that after completing 1-year training course, only 80% of the possible findings were seen by students.

Consequently, every day, medical staff are asked to make a diagnosis from US images without appropriate training.

To overcome these difficulties and improve training efficiency, scientists have introduced simulation technique as a new way of training, where neither patients nor US equipment are needed. In 1968, one of the earliest medical simulators for trainees was created by the University of Miami, Miami, Florida, USA. This animated mannequin to teach cardiovascular disease could perform more than 27 cardiac functions of the human body (Gordon 1974). In the next generation of simulators, interactive models were developed that responded to actions taken by a physician for fibre-endoscopic training (Gillies and Williams 1987). The last generation of medical simulators were computer based, able to reproduce touch and force feedback feelings using specific joysticks such as the phacoemulsification simulator (Lam et al. 2014). However, the proposed systems lacked the immersive environment for the learner, especially, regarding the US image deformation and force feedback feeling.

Currently, learning is conducted based on newest technology developments to overcome the pitfalls of the traditional learning process. These modern learning techniques are typically based on the simulation of the real, learned and expert gestures. Upon a survey of the existing simulators (Ourahmoune et al. 2012) for learning US gestures, two kinds of simulators interest the scientific community:

- (i) Simulators with physical plastic model and a false US probe equipped with a localiser which receives the 3D relative position and orientation of the probe (Stallkamp and Wapler 1997; Aiger and Cohen-Or 1998; Maul et al. 2004; Weidenbach et al. 2004, 2007; Breikreutz et al.

2009; Persoon et al. 2010; Lertwiram et al. 2011; Sun and McKenzie 2011; Liu et al. 2015).

- (ii) Simulators that are based on biomechanical modelling of the studied anatomical part; these models assume that the entire region has the same elasticity while it is actually heterogeneous (Ehricke 1998; Arkhurst et al. 2001; Aulignac et al. 2006; Vidal et al. 2008; Sclaverano et al. 2009; Goksel et al. 2011; Petrinc 2013; Pirkowski and Kempny 2013; Williams et al. 2013; Peters 2014).

As far as the simulated 2D US images are concerned, two approaches exist in literature. The first is generative approach that synthesises US texture using methods based on a ray tracing model (Jensen 1996) and methods based on a linear convolution model (Bamber and Dickinson 1980), both using a geometric anatomical model as reference. This approach lacks the simulation of artefact, blurring effects and other US image specifications. This approach can be used in cases of dynamic structures, but it is time-consuming (Aiger and Cohen-Or 1998).

The second is interpolation approach (Rohling et al. 1999) based on using the 3D US volume acquired off line from real patients. Even if it is widely used and is quite fast to be used in real time, it needs to choose the optimal interpolation technique, and it is not adapted for complete dynamic structures.

Alessandrini et al. (Alessandrini et al. 2015) introduced a novel pipeline for the generation of synthetic 3D cardiac US image sequences and generated an open-access database. A freehand foetal US simulation method based on spatially conditioned generative adversarial networks was presented (Yipeng et al. 2017), and the US acquisition was performed using an US probe tracked by an optical tracker on an anatomical realistic foetus phantom. Storve and Torp (2017) simulated US images that have the essential noise characteristics of real US. In another hand, Storve and Torp proposed highly efficient parallelised central processing unit and graphics processing unit implementations of the COLE algorithm (Gao et al. 2009) with an emphasis on dynamic simulations involving moving point scatterers.

US image deformation is a complex phenomenon and is typically not allowed in most existing simulators. The deformation of the image, when pressure is applied, can be obtained based on segmentation of the non-deformed US image (Henry 2009). The deformation of tissue areas is calculated by taking into account the pressure parameters. Alternatively, a deformation function can be calculated directly from the position of features on a deformed and non-deformed image. Aulignac and colleagues (Aulignac et al. 2006) proposed to deform the US image only in linear manner, not corresponding to the non-linearity deformation of the anatomical structures. For the mannequin-based simulators, the plastic used has elasticity completely different from that of the human structures. For the virtual simulators, the biomechanics models based on Hooke's law using finite-element modelling domains and spring-mass models adapted by Aulignac and colleagues (Aulignac et al. 2006) simulate the non-linearity of the anatomical structure but not the elastic heterogeneity. To match the frequency of the force feedback joysticks, the models are simplified so that they can generate non-realistic force feedback. In order to obtain real-time

systems, many improvements have been achieved to reduce processing time based on continuous adaptive haptic rendering (El-Sana and Varshney 2000), force interpolation for real-time force feedback rendering (Zhuang and Canny 2000; Mazzella et al. 2002), physically based simulations (Weller and Zachmann 2009), graphics processing unit (Courtecuisse et al. 2010), multi-threading (Peterlik et al. 2011) and optimisation (Wang et al. 2013).

Remote US exam was proposed by Delgorgue et al. (2005) using a robot that held an US probe and provided information of the force applied through the probe on the patient, using force sensors mounted on the probe. However, this could only be achieved using a robotic arm and not with a free hand.

Table 1 provides an overview in terms of features and immersion for the existing simulators. Based on this, we could conclude that existing simulators lack learners' immersion as far as US image deformation and force feedback simulation are concerned. They are focused on US image simulation, and learning process is typically ignored. Furthermore, existing simulators are of high cost, which constitute a barrier to their diffusion and large-scale use. The simulators with plastic mannequin and dummy probe used a 3D localiser in simulation phase which is expensive, and as for the virtual simulators the force feedback joysticks used are again expensive, making them unsuitable for learning process.

On the other hand, virtual environment for training including intelligent tutoring system has also been proposed in the literature. For example, Santos and Osrio (2004) explored the educational uses of virtual learning environment, whereas Rickel and colleagues proposed an intelligent agent that assists the user in intelligent virtual environment for process training (Rickel and Johnson 1999; Pan et al. 2006; Xu and Wang 2006).

This leads us to propose in this article a new approach to design an US virtual environment, considering affordability impact on virtual environment usability (Shin 2017). In this study, a virtual immersive environment which simulates US examination for efficiently learning the US technique with all the human senses is proposed. Section 2 is devoted to a detailed description of the proposed method and material for US probe localisation and force feedback measure and explains how the learning database for US musculoskeletal application is built and the use of the acquired data to design a virtual environment. The evaluation of this new learning tool is presented in Section 3, followed with a discussion in Section 4. A conclusion and some improvement perspectives are given in Section 5.

2. Materials and methods

The cost of the proposed virtual environment is low because it uses a force feedback joystick (see Figure 1). The virtual environment simulates US images as well as US image deformation and includes a realistic force feedback simulation. In addition to simulation, an intelligent agent autonomous from the human expert is involved to supervise the learner in the learning process, which would be a good gesture and reproduce expert guidance. A report of learning outcomes would be returned to the expert and synthesised by an intelligent

Table 1. Existing simulators. BR: Body representation, PR: Probe representation, IMM: Immersion, DOF: Degrees of freedom, MS: Motion sensor, D: Data, ARFF: an realistic force feedback from plastic mannequin, NFF: No force feedback, DP: Dummy probe, MQ: Mannequin, VB: Virtual body, VP: Virtual probe, US: Ultrasound, Nol: No information available.

Simulator	Data	BR	PR	IMM
UltraTrainer (Stallkamp and Wapler 1997)	3D US D	MQ	DP 3D MS	ARFF
UltraSim (Aiger and Cohen-Or 1998)	3D US D	MQ	DP 3D MS	ARFF
SonoSim3D (Ehrlicke 1998)	3D US D	VB	VP	NFF
Paediatric simulator (Arkhurst et al. 2001)	3D US D	VB	VP 2DOF	NFF
SonoTrainer (Maul et al. 2004)	3D US D	MQ	DP 3D MS	ARFF
Echocardiography simulator (Weidenbach et al. 2004)	3D US D	MQ	DP 3D MS	ARFF
Thrombosis simulator (Aulignac et al. 2006)	3D US D	VB	VP 3DOF	ARFF
TransEsophageal Echocardiogram (Weidenbach et al. 2007)	3D US D	MQ	DP 3D MS	ARFF
US-guided needle puncture (Vidal et al. 2008)	CT image	VB	VP	ARFF
Schallware (Breitkreutz et al. 2009)	3D US D	MQ	DP	ARFF
US-guided biopsy (Sclaverano et al. 2009)	3D US D	VB	VP	ARFF
TRUS (Persoon et al. 2010)	3D US D	MQ	DP 3D MS	ARFF
Obstetric ultrasound simulator (Lertwiram et al. 2011)	3D model		DP 3D MS	ARFF
US-guided needle puncture (Goksel et al. 2011)	CT image	VB	VP	ARFF
				NFF
Echocardiogram simulator (Sun and McKenzie 2011)	LC	MQ, VB	DP 3D MS, VP	ARFF
SonoSim3D (Petrinec 2013)	3D US D	VB	VP	NFF
Web-based TransEsophageal Echocardiogram (Pirkowski and Kempny 2013)	CT image	VB	VP	NFF
Scan trainer (Williams et al. 2013)	Nol	VB	VP	Nol
Web-based TransEsophageal Echocardiogram (Peters 2014)	CT image	VB	VP	NFF
Obstetric US simulator (Liu et al. 2015)	3D US D	MQ	DP 3D MS	ARFF

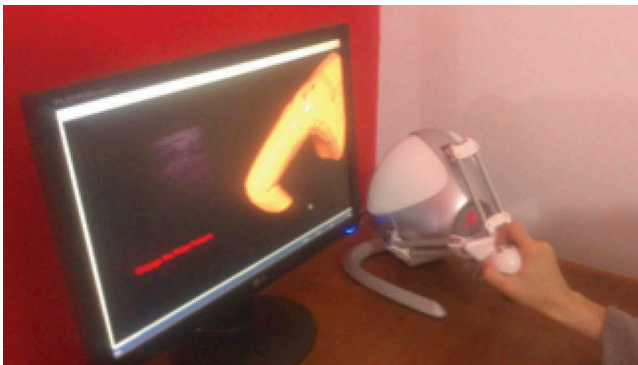


Figure 1. Learning virtual environment: Joystick as a probe, US image corresponding to the position, orientation and applied force through the joystick, dialog window to help the learner.

agent, which allows making decision in debriefing step about learners' performance.

Our contributions in this article as described in the flow chart (see Figure 2) are:

- A lightweight US probe instrumentation to acquire real-time US image pose and applied force. The instrumentation is designed for freehand use (detailed in Section 2.1).

(i) Construction of the elasticity map for the anatomical region of the studied organ (detailed in Section 2.2.1).

(ii) Acquisition of the US volumes for the subject organ at different force levels (detailed in Section 2.2.2).

(iii) Identification and US image acquisition of reference with the associated probe pose and the applied force (detailed in Section 2.2.3).

The acquired US learning database allows:

(i) Simulation of the force feedback by using the acquired elasticity map translated to the learner by a force feedback joystick adapted to learning (detailed in Section 2.3.1).

(ii) Simulation of US images and deformation by using interpolation based on the database of 2D US images (detailed in Section 2.3.2).

(iii) Supervising the learner by the intelligent agent, making use of the acquired information for the US images of reference and keeping the expert informed of the learning results by the intelligent agent (detailed in Section 3).

2.1 Ultrasound probe instrumentation

In order to acquire an US volume of the studied body part and to develop the elasticity map of the region of interest, the US probe pose was determined and the force applied to the probe was measured continuously during the US gesture. Our targeted clinical application was the exploration of musculoskeletal body part. These structures were characterised by their complexity and the heterogeneity of their elasticity component structures.

2.1.1 Localisation

The 3D localisation and orientation of the probe was acquired using an NDI Spectra Polaris localiser (Northern Digital Inc. International Headquarters Waterloo, Ontario, Canada). We equipped the US probe with a rigid body (the referential system of the probe) visible by the camera as illustrated in Figure 3 (encircled by a red ellipse) (Ourahmoune et al. 2014). Before the use of the proposed instrumentation, the US probe

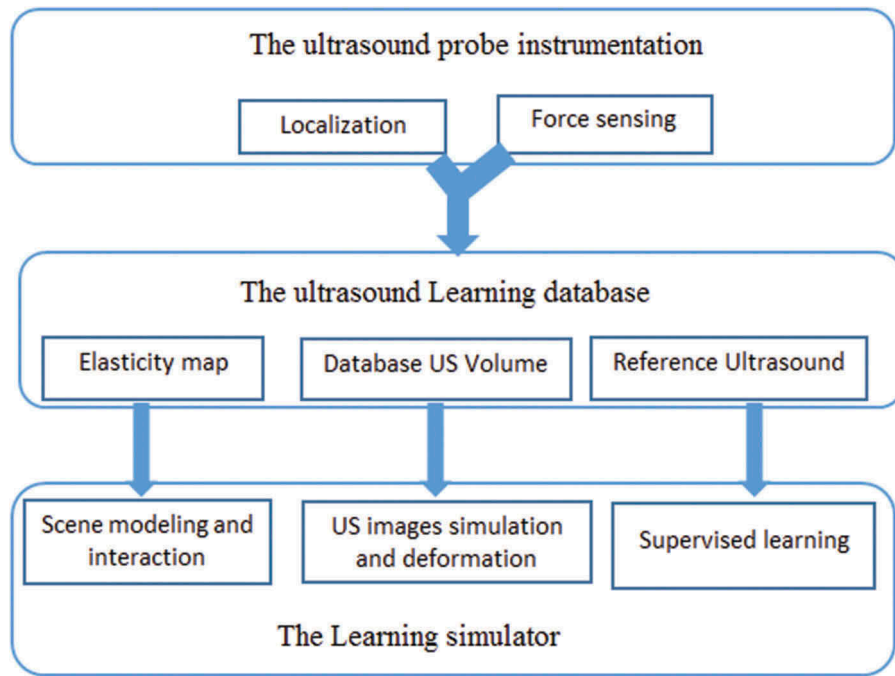


Figure 2. Pipeline for the proposed learning environment.

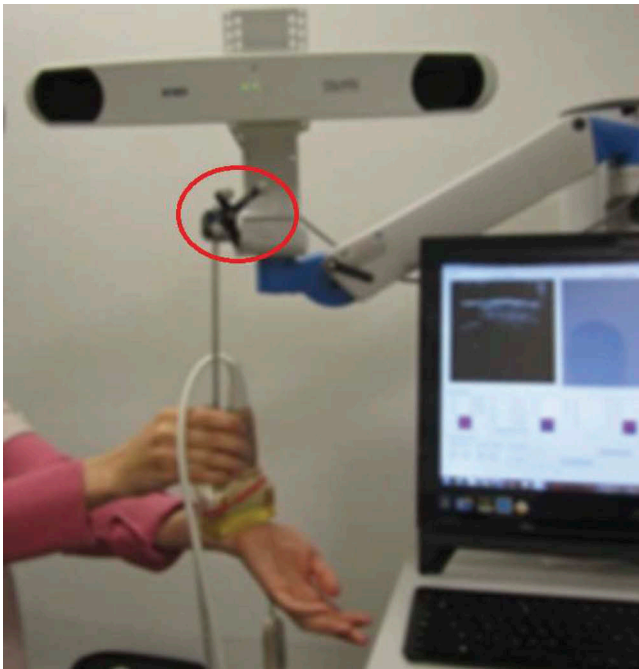


Figure 3. The US probe with its attached rigid body (encircled in red) and the used optical localiser.

was calibrated using the calibration procedure developed by Chaoui et al. (Chaoui et al. 2009). This new concept (patented) (Dardenne et al. 2008) for freehand US calibration method was fully automatic and was based on the probe virtual movement simulation. This optical localiser provides in real time the pose of the probe. For each pose, the US image and the associated pose of the probe were recorded, creating a complete database for reference data.

2.1.2 Force sensing

To acquire the applied force on the US probe during the acquisition, we instrumented the probe with two force sensors, one at each side of the proximal US probe area (see Figure 4). Force information was collected using force sensors wired to a computer without altering the US waves and without disturbing the force acquisition process. The FlexiForce sensor (ELF Economical Load and Force, Tekscan, Inc. South Boston, MA, USA) was selected as it was the most appropriate sensor for this application. This sensor has an accuracy of $\pm 3\%$ and offers the advantage of being very thin, its thickness does not exceed 0.1 mm and it has a circular sensitive area which does not exceed 0.6 of diameter (Hollinger and Wanderley 2006). The force range of this sensor was from 1 N to 100 N. This range corresponded to the variation of force applied through an US probe to anatomical regions. The minimum force value was applied in articular exams, while the maximum value was applied in abdominal exams. We first calibrated the sensors for a maximum value of 5N (Delgorge et al. 2005; Aulignac et al. 2006). This value was determined by a clinician to be the maximum force applied through the probe when scanning human articulations.

The sensors were placed on the probe so that all the force applied on the probe passed through the sensitive area of the sensors. Sensors were placed in such a way that they did not influence the transmission-reception process of the US waves. To ensure that all the applied forces to the US probe passed through these two sensors, we added two very thin plates with 1 mm of thickness and 5 mm of diameter, one for each sensor. US probe had an opening area of 6060mm by which the US waves pass through, and by adding the two plates, the opening area remained unobstructed for more than 50 mm which was large enough to acquire a good US image (see Figure 4).

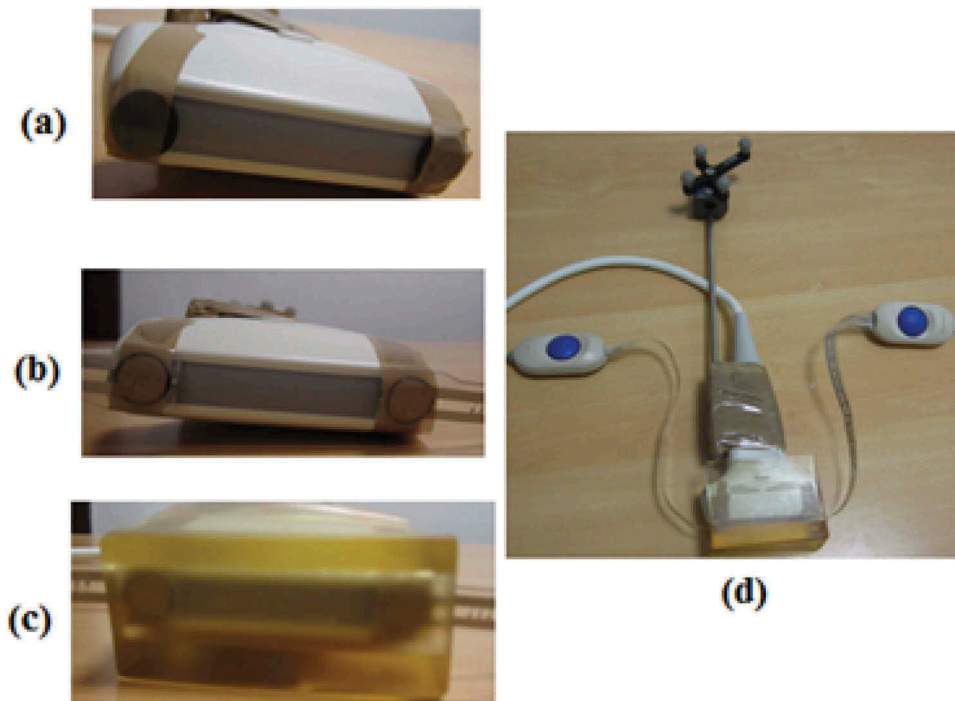


Figure 4. (a) Probe instrumented with the plates, (b) instrumentation supplied with the sensors, (c) instrumentation supplied with the pocket and (d) complete instrumented probe.

The probe, the plates and the sensors were placed in a pocket in Proxon (Mantke and Peitz 2011); which is an extremely soft polyvinylchloride material created especially for the requirements of skin contact sonography. This material exhibits characteristics similar to human tissue in its sonic velocity, sound absorption and acoustic wave resistance. It was suited for our case study due to its low sound absorption. The probe protection was made for a linear probe and it was 70 mm length and 10 mm of thickness. This cover had the same form as the probe and ensured that the force was applied on the entire contact area, making the same deformation of the underlying tissues as that of the probe. It allowed a good US transmission. We ensured the conductivity of US waves with US gel between the probe and the probe cover.

The force sensors were calibrated before being used. The maximum force applied in musculoskeletal structures is about 5N. This value was obtained using a scale on which the expert applied the maximum force usually applied on musculoskeletal organs with the US probe. The sensors were first saturated with this maximum force value and then calibrated by the mean of the calibration tool provided by FlexiForce application (Hollinger and Wanderley 2006) (see Figure 5).

As shown in Figure 5, the two sensors returned the same force F_1 (force returned by the first sensor, entry COM8) and F_2 (force returned by the second sensor, entry COM9) and the resultant force was the same for the two sensed forces. This was due to the piezoelectric characteristic of the used sensors. The force feedback F_{app} was equal to the applied force F_{rec} in

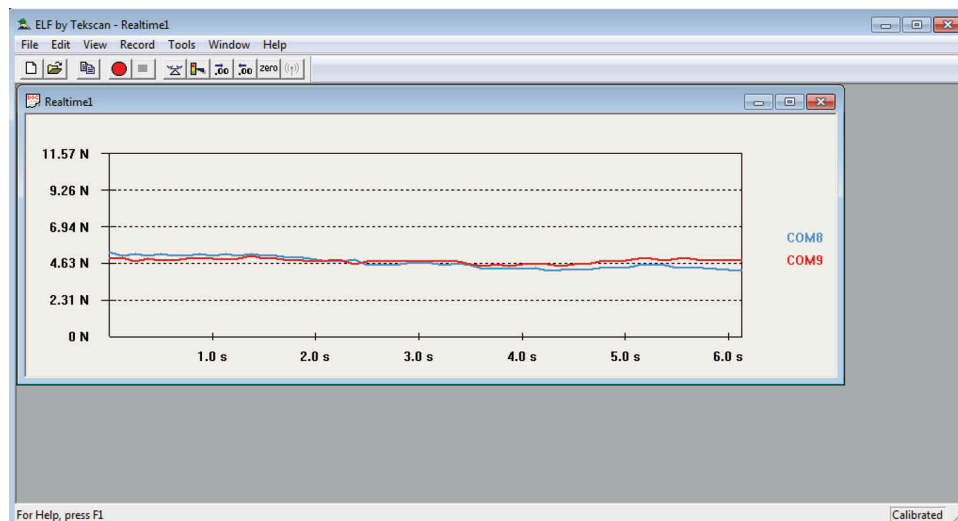


Figure 5. Signal force representation of the two used force sensors from the USB-connected port com9 and com8.

magnitude and in opposite direction (see Equation 1). The non-strait signal representation was due to the deformable anatomic structures.

$$F_{app} = -F_{rec} = (F_1 + F_2) \div 2 \quad (1)$$

2.2 The ultrasound learning database

2.2.1 Construction of the elasticity map

When performing the US exam, clinicians aim to get a good US image of the organ of interest. Thus, they move the US probe by applying a force through the probe on the region related to the studied organ. In order to well simulate the US exam, we measured the required applied force to acquire each US image. To ensure the US wave transmission reception, the use of gel is imperative and it further reduces the frictional forces. As anatomical tissues are isotonic, the range of the reactive force F_{react} remains the same when the probe orientation varies. Therefore, the reacting force has the same amplitude, while the applied force F_{app} is in the opposite direction.

The 3D positions of points of tissue were computed for different force levels. Using this data, we were able to recover the forces for each indentation using an interpolation method. Moreover, we noticed that the deformation of the tissues was different from one point to another; uniform biomechanics models were not close to reality.

2.2.2 Reconstruction of the ultrasound volume for the studied organ

The musculoskeletal structures of used shoulder articulation are complex and heterogeneous. For this study, the expert clinician performed the US exam using the described acquisition protocol on healthy male volunteer.

Once the sensors were calibrated, the localiser provided the position of every pixel of the US image. We assimilated the position of the probe to the position of the first pixel of the US

image in order to reconstruct a 3D US volume of the shoulder from a set of 2D acquired US images.

To acquire the US exploration of the studied organ, the expert defined the area of interest; we acquired at each point of the region of interest an US image and registered the position and force information. The acquisition points were 1mm equidistant from each other (example images are presented in Figure 6). This distance was chosen after several tests and it allowed us to reconstruct an optimal US volume. For each force range, a set of US image of the shoulder was associated.

For each point of the area of interest, we acquired three US images associated with the force applied to the probe during its acquisition. We obtained an US volume for each force variation, and US volumes then contain the information on the deformation of the anatomical structures of interest. Once the learning database was constructed, the US volumes with the elasticity map were used to supervise the learner.

2.2.3 Identification and storage of the reference ultrasound database

A reference exam was considered to be the one with all US images that held relevant information of the studied organ. For an US exam, it was important to know where the US probe was placed to begin the exam; this location was different from one organ to another. For each US image of reference, the position and the orientation of the probe in addition to the necessary force for image production were saved with the associated US image. This information was used to supervise the learner during the learning process.

2.3 The learning simulator

The US images were taken from a real patient. Deformations were simulated by interpolation over the three US volumes, and a realistic haptic feedback was calculated by interpolation on the registered elastic data.

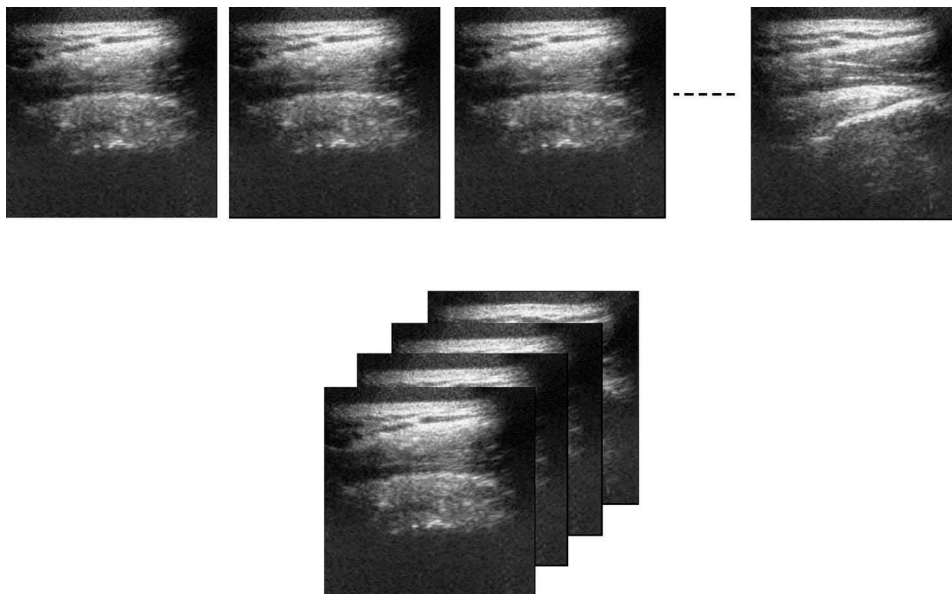


Figure 6. Sets of ultrasound images for the global ultrasound volume reconstruction.

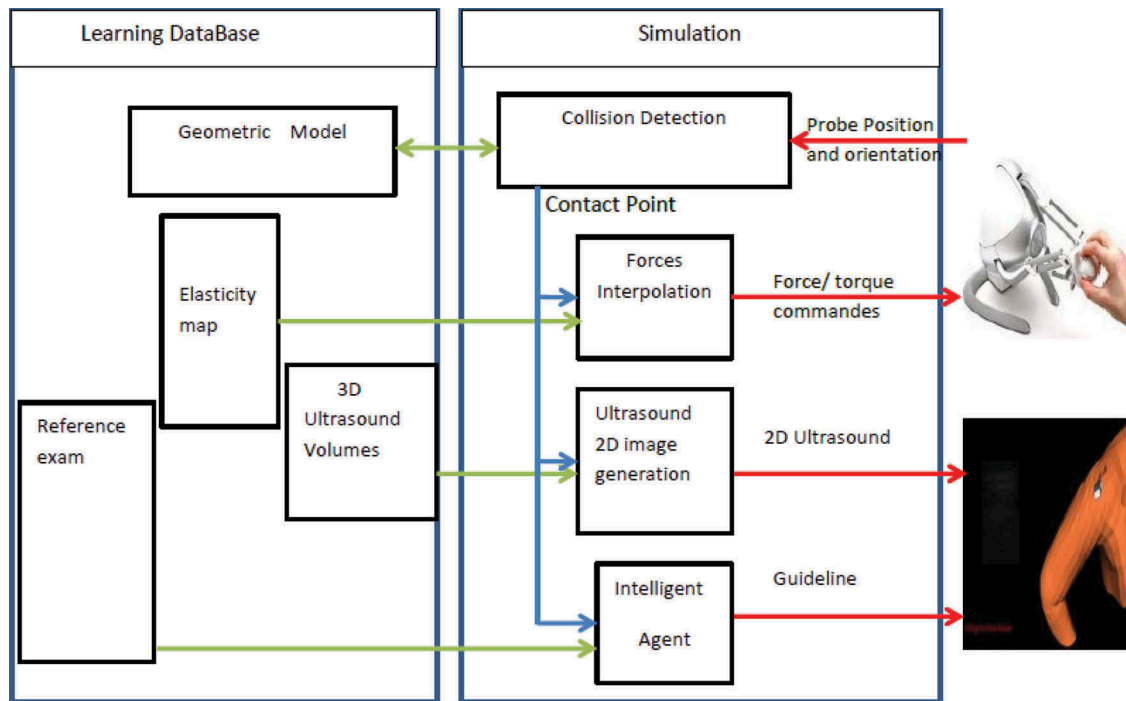


Figure 7. Graphical overview of the learning simulator.

To design the virtual environment, we considered three steps:

- (i) Geometric modelling,
- (ii) Interaction design, and
- (iii) Supervised learning

A graphical overview of the system is illustrated in Figure 7.

2.3.1 Virtual scene modelling

The virtual environment integrated two objects, a virtual US probe and a virtual model of the patient. The virtual US probe was a geometrical shape constructed using a set of points (vertices) and facets. The virtual patient model was a polygonal model constructed from anthropological data of human. For purposes of convenience for the learner, we presented the virtual model that simulated the patient trunk. However, only the region of interest corresponding to the explored organ (supraspinatus tendon) was treated which was the workspace of the learner and it was deformable when the rest of the model was not. Only the working space allowed the interaction with the virtual probe. During the acquisition phase, we built a database for learning US gesture. To properly use the training set, it was necessary to calibrate this data with the virtual scene. This calibration amounted to a change of scale between the acquisition area and the virtual workspace.

Interaction. An US exam was performed by passing the probe on the patient in contact with the skin at different force levels. The use of enough gel ensured the maximum and uninterrupted transmission reception of the US waves. We assumed that the virtual probe moved on the surface of the

model without the use of friction forces, while the US gel in the actual configuration eliminated any frictional force present. As a result, the interaction between the virtual model of the patient and the probe resulted in contact and indentation. This was to show how the virtual probe interacted with the virtual model.

Collision detection. To detect the interaction between the virtual US probe and virtual patient model, we chose to use a collision detection method using a hierarchical oriented bounding boxes (OBBs) (Gottschalk et al. 1996). It is known that collision detection algorithms are computationally expensive, so an OBB was calculated only on the region of interest to save computational time. A collision was detected if a point of the virtual probe intersected with the OBB from the area of interest.

Collision response. Following a collision, two types of response occurred in our case study. The first response was visual (graphical) that resulted in a deformation of the patients' polygonal model, generation of the US image and its deformation. The second one was haptic and translated the force feedback. We used the method of the proxy (Zilles and Salisbury 1995) to calculate the distance between the probe and the collision point. It is known that biological tissues have a non-linear distortion due to the heterogeneity of the elasticity of the component structures and the non-uniform distribution of the latter. But in our case, the supraspinatus was in a superficial region and the deformation was minimal due to the non-deformation characteristic of the bone.

Haptic response. To make a haptic and graphic perception in one simulation cycle in a virtual reality interaction simulation on deformable object, solutions based on force interpolation

have been proposed. Zhuang and Canny (2000) obtained force feedback by interpolating between simulated states. Mazzella et al. (2002) used a force grid data structure for the haptic force interpolation and extrapolation.

To provide a smooth haptic force feedback and allow the haptic device to render force feedback in a higher update rate, we proposed to take advantage from the elasticity map registered in the learning database. The virtual workspace was divided into mesh points. Each vertex kept the registered force feedback.

We assumed that at each point the tissue had piecewise linear characteristics because of its own elasticity. When a collision occurred between the virtual probe and the virtual region of interest, force feedback was calculated. Based on the position of the manipulator tip, the force feedback on each collision point was simulated by interpolation between the forces on corresponding points in the two closest force levels. We selected the nearest two vertices to the collision point in the two force levels $P_1(Z_1, F_1)$ and $P_2(Z_2, F_2)$; the force feedback F_i at $P_i(Z_i, F_i)$ given by Equation 2 was a piecewise linear interpolation between the two selected forces. In case the collision point matched with a vertex in a force level, the force feedback was the force at this vertex (see Figure 8).

We noted d_i as the distance from force level mesh point i , $i = 1, 2$.

$$F_i = F_1 + (F_2 - F_1)(Z_1 - Z_i)/(Z_2 - Z_1) \text{ if } \exists d_i \neq 0 \text{ else } F_i = F_{\text{vertex}} \quad (2)$$

This approach allowed a considerable saving in computational time and more faithful result than the biomechanics models without any acceleration and simplification supplied. It permitted to manage different update rates between the visual loop and the haptic loop. The haptic engines were transmitted to the user by the means of a haptic interface. We choose to use the Falcon Novint technology joystick force feedback (Martin and Hillier 2009); this joystick offers three degrees of freedom and maximum force feedback of 9 N, this joystick combines the best features and its cost is adapted to learning. Figure 9 is a side view schematic of one of the three kinematic chains. The subscript i denotes the i^{th} kinematic

chain, where $i = 1, 2, 3$. The origin (the centre of the stationary platform) is labelled point O , and the centre of the moving platform is labelled point P . p is the vector from the centre of the stationary platform to the centre of the moving platform. The distance from the centre of the stationary platform to the lowest joint (joint A_i) is denoted r , and the distance from the centre of the moving platform to the highest joint (joint E_i) is denoted c . The lengths of the links are labelled a, b, d and e . The angular positions of links A_i, B_i and C_i are given by θ_{1i}, θ_{2i} and θ_{3i} , respectively. A coordinate frame (u_i, v_i, w_i) is defined for each kinematic chain, attached at point A_i (Block et al. 2013).

2.3.2 Ultrasound image simulation

Volumes reconstruction. From the acquired US image sets in the first step, we reconstructed a 3D US volume of the shoulder by applying a linear interpolation algorithm (Lehmann et al. 1996). Image interpolation based on grey-based interpolation was the most common and simple method. From the US volumes acquired offline, we could generate US slices of any position and orientation in real time (see Figure 10).

Ultrasound image deformation. In human body, typically, superficial soft tissues have a near linear deformation, while deep tissues and bones have negligible deformation. The main difficulty in modelling the US image deformation lies in the fact that each structure has its own way of reacting under pressure (see Figure 11). Therefore, simulating US image deformation under pressure is a delicate process and most of the existing simulators do not simulate it.

We proposed to use nearest neighbour interpolation algorithm (Lehmann et al. 1999) between the reconstructed volumes to realistically simulate deformation on the US image. This gave us a continuous render of the US images for each US gesture. Identification of a new grey value of image pixels needed to use the information of corresponding points on other slices of grey level. Assuming the known US image $I(x_i, y_j, z_k)$ and $I(x_i, y_j, z_{k+1})$ interpolation between them provided new image $I(x_i, y_j, z)$ such that:

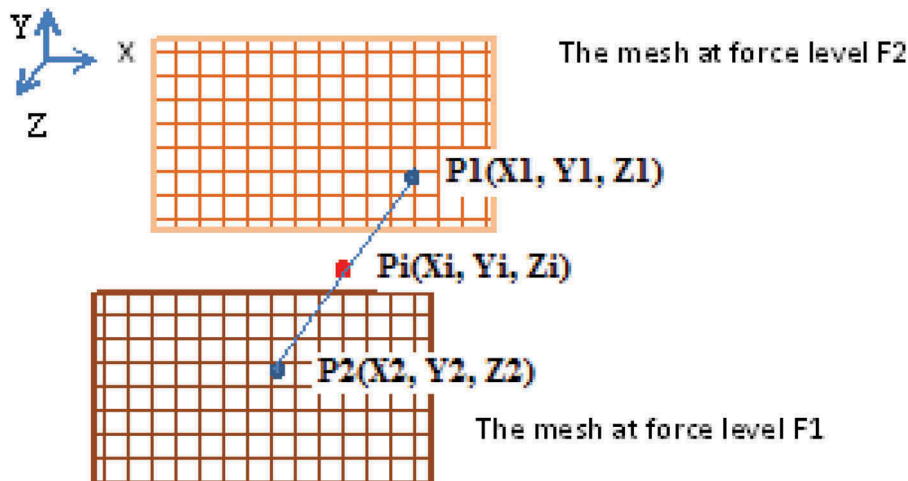


Figure 8. Force interpolation between two successive force levels.

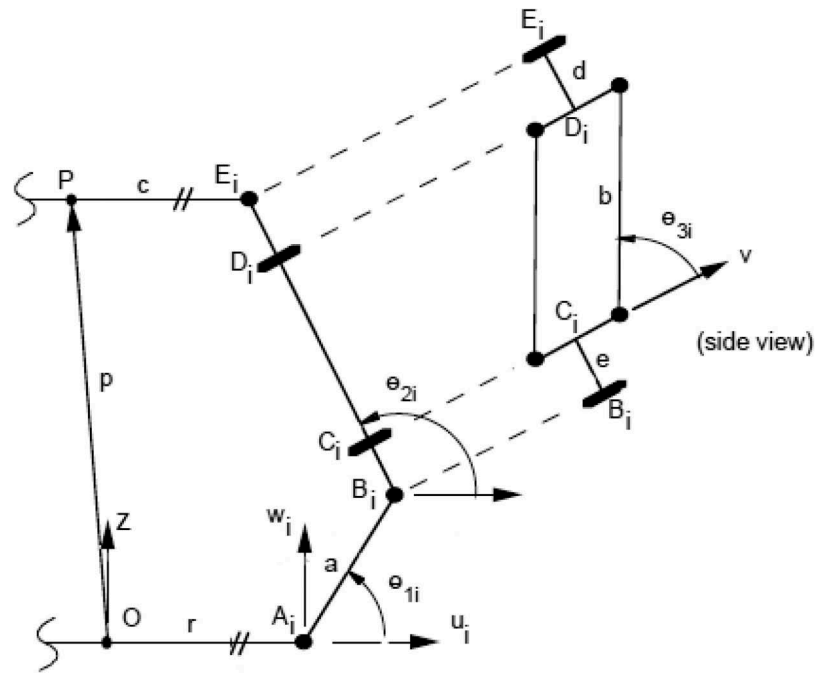


Figure 9. A side view schematic of one of the three kinematic chains (Block et al. 2013).

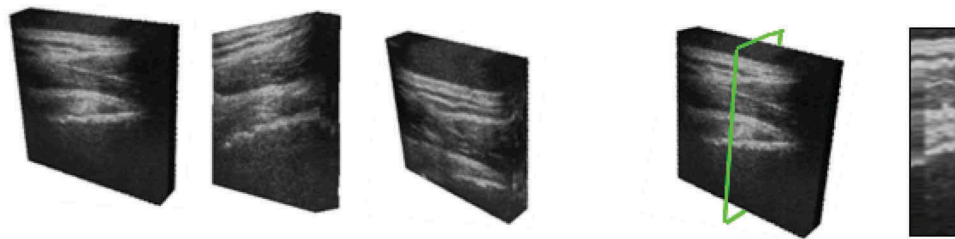


Figure 10. (Left) Ultrasound volumes rendering at different force levels. (Right) Image at a different slicing plan.

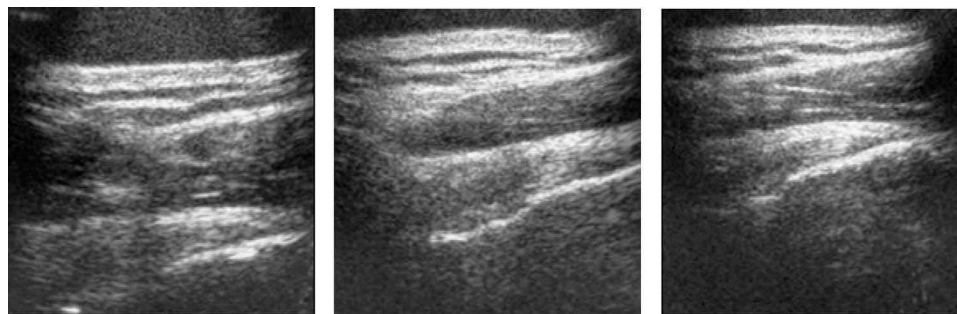


Figure 11. Ultrasound image acquired with three force levels.

$$I(x_i, y_i, z) = I(x_i, y_i, z_k) \text{ If } z - z_k < 0.5 \text{ otherwise } I(x_i, y_i, z) = I(x_i, y_i, z_{k+1})$$

Ultrasound image segmentation. Because the US exam does not give direct correspondence to anatomy, it is hard for the beginners to identify the anatomical structures in the US image. Therefore, we gave the learner the possibility to identify each region in the rendered US image. The US image was segmented automatically in real time; as a result, the US

image regions were labelled. This made the learner understand the image component at each acquisition level during the exam and allowed good anatomical positioning of the US probe.

For the supraspinatus US exam, the anatomical region of interest included following components in anatomical – order skin and fat tissues, deltoid muscle, supraspinatus tendon and the head of the humerus. Each structure is characterised by a special US appearance. The bone contour was characterised by a high echogenicity (high-intensity pixels). The tendon is

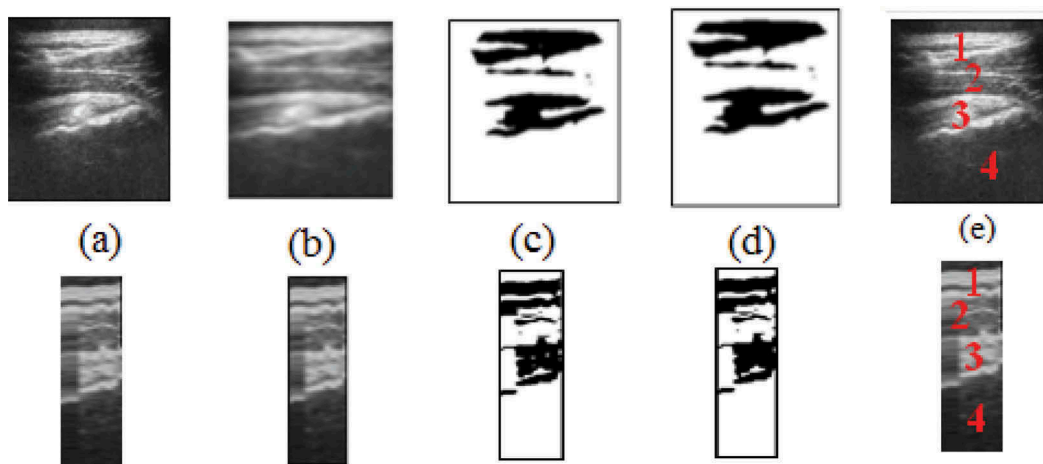


Figure 12. Segmentation steps and results for two different image plans (axial and transversal plans): (a) initial image, (b) smoothed image, (c) thresholded image, (d) dilating and eroding, (e) result of segmentation where 1: skin, 2: deltoid, 3: supraspinatus, 4: humerus head, (f) hand-drawn regions by the expert where S: skin, D: deltoid, SE: supraspinatus, H: Humerus head.

echogenic and fibrillary. Muscle is lower echogenicity. Skin and fat are high echogenicity because they are superficial structures.

Using this information of anatomy location and US appearance, a segmentation method was proposed. This method works only in simulated and environment-controlled situations. US image segmentation is known to be a hard work due to its specular appearance; therefore, we first needed to reduce the noise of the image. For that purpose, we chose to use the Gaussian smooth filter. In the second step, we applied a threshold to select higher intensity pixels and finally we applied a dilatation and erode filters to connect the closest components and eliminate small and parse ones.

Using the anatomic characteristics, we identified the regions in the segmented image. We knew that the first region in the image was relative to the skin and fat because it was a superficial region and we knew that the lowest region was close to the tendon region. The head of the humerus was just under the tendon region and the deltoid muscle was situated between the tendon and the skin. This way we identified all the structures and extracted their location. We added labels to the original US image for the identified regions relative to the localisation. The segmentation results were evaluated comparatively to a manual segmentation done by the expert and presented in Figure 12. However, the proposed segmentation method was tested only in a simulated environment and works only in controlled situations.

2.4 Supervised learning

In the traditional learning process, the trainee is typically asked to perform the US exam on a patient guided by the expert as expressed in Driscoll and colleagues (Driscoll 2007). This is why in the proposed learning solution an intelligent agent was included to guide the trainee in the simulation step. According to Levine et al. (2013), the adapted Kolb's cycle for healthcare includes simulation, supervision

and outcomes, and a direct supervision is implicated on debriefing after simulation using outcomes. Therefore, in the proposed solution, the trainee simulations were stored and used by the expert in the debriefing step to identify trainee errors in the gathering step of the three-step debriefing model (gather, analyse and summarise). In the acquisition phase, we recorded a reference exam of the studied organ. A reference US image held pertinent information. For all reference US images, we knew their positions, orientation in our virtual environment (after calibration) and the necessary pressure.

Using all this information and taking advantage of the educational agent technology (Payr 2003), two simple intelligent agents were implicated (see Figure 13). The first one was a pedagogic agent (acts as a tutor) completely autonomous from the human expert. It was able to guide the learner and ensure a good learning experience. The pedagogic agent observed the learner's actions, the main function compared the manipulation of the learner to the next reference image and it assisted the learner by indicating proper handling at the end to find the right US image. The pedagogic agent started by showing the learner the first position of the probe as a good start. The intelligent agent used the supervised learning function to guide the learner. Figure 14 illustrates the virtual environment at different errors of probe manipulation.

All the learning results were stored and reported to the expert in the debriefing phase. The results were synthesised and displayed in the chart for data visualisation by a synthesiser agent. It kept the expert informed of the learners' performance and allowed him to make decisions.

3. Evaluation

Evaluation of the system usability and measurement of user experience in a virtual training environment was essential (Shin et al. 2013; Shin 2017). A group of 120 participants, 60 experts and 60 first-year students of radiology and rheumatology,

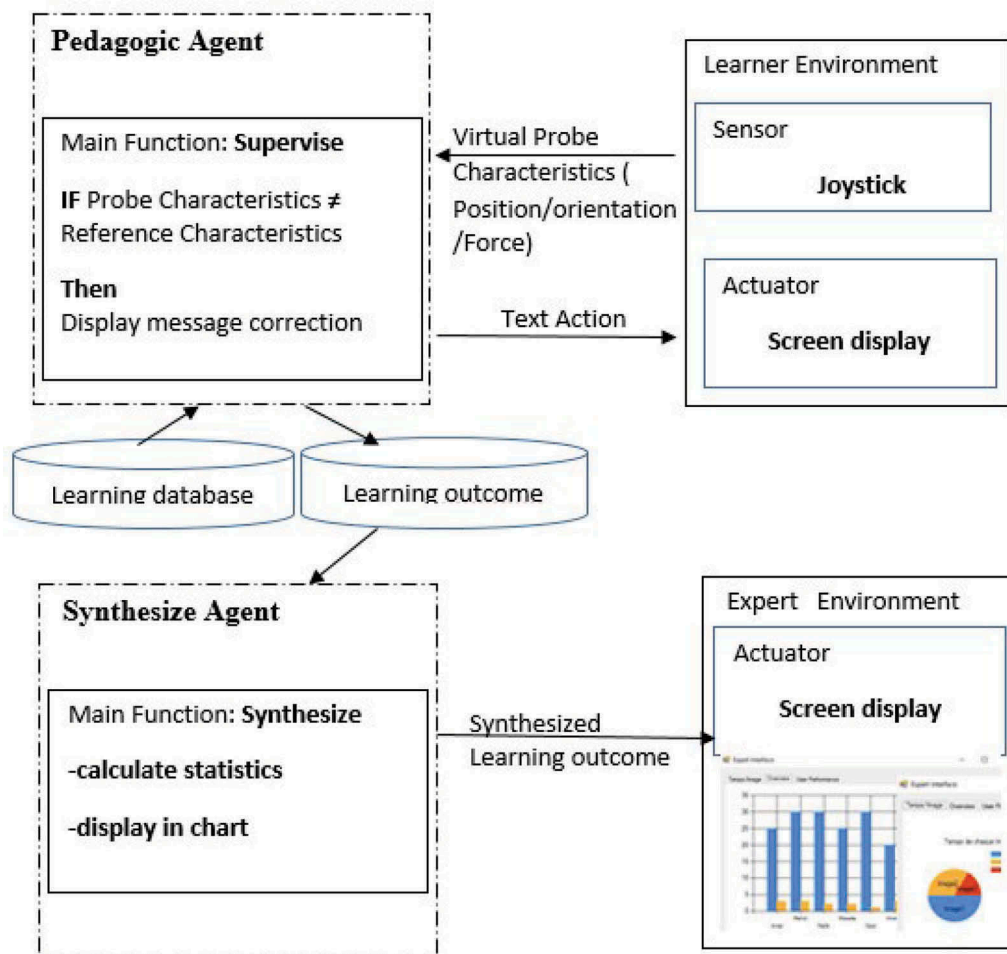


Figure 13. Intelligent agent system for the proposed learning environment.

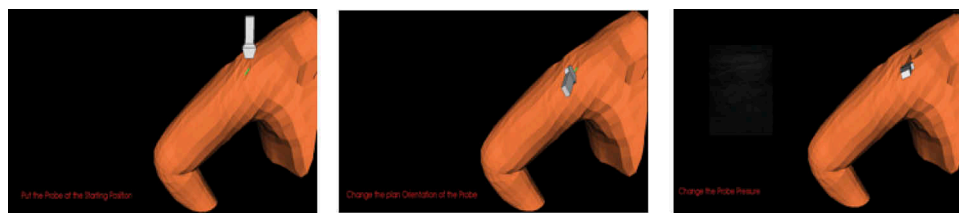


Figure 14. Supervised learning: From left to right: incorrect position, incorrect orientation, incorrect force.

used our virtual environment. An evaluation was performed based on the survey of US simulator evaluation (Sidhu et al. 2012) and the consensus guidelines for validation of virtual reality surgical simulators (Carter et al. 2005). Face, content, construct and transfer validity were conducted. Statistical results were performed using ANOVA (analysis of variance) data analysis method.

3.1 Face validity

Immersion, interaction and perception, which form the basic aspects of a virtual environment (Fuchs et al. 2011), were evaluated. A scoring system, with scores in the integer range

1–10 (the higher, the better), to subjective aspects of the simulator was adapted.

The experts evaluated the haptic perceptions related to haptic device in terms of sensations, force intensity and degree of freedom. Also, the subjective perception of spatial and temporal coherence between visual and haptic stimulators provided by the system during the simulation is evaluated.

Scores were given to:

- (i) US image quality,
- (ii) US image deformation,
- (iii) Credibility of interactions,
- (iv) Force feedback intensity,

Table 2. Face validation scores.

Aspects	Average score	Variance
Ultrasound image quality	9.19	0.21
Ultrasound image deformation	8.87	0.28
Credibility of interactions	8.10	0.03
Force feedback intensity	8.67	0.18
Probe manipulation	7.22	0.08
Perception of spatial and temporal coherence	8.21	0.07

Table 3. Construct validation.

Groups	Count	Average time (min)	Variance
Expert	60	5.59	0.53
Learner	60	14.33	2.21
F		P	
1.99E+ 03		1.14E-75	

- (v) Probe manipulation,
- (vi) Perception of spatial and temporal coherence.

Obtained results are presented in Table 2.

3.2 Content validity

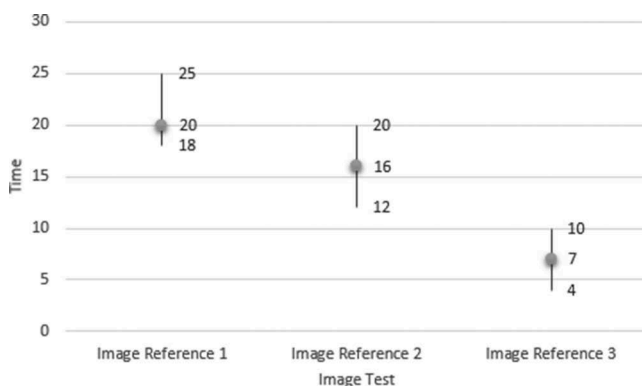
In the first step, the learners were asked to find three US images of reference supervised by the intelligent agent. Time to retrieve each US image was the criteria for evaluation.

The US image of reference was retrieved during an average time of 20 min for the first US image of reference. However, for the third, the reference image was retrieved in 5 min as shown in Figure 15.

In the second step, the trainees were asked to perform the US exam without the supervision of the intelligent agent, and we added the retrieval of the US image reference as an evaluation criteria. For all trainees, the US exam including all image references were performed within a time out of 30 min (30 min is an average time duration of an US exam). Only one learner had gone over this time by 6 min and two other learners designated a wrong US image.

3.3 Construct validity

In this step, the ability of the virtual environment to differentiate between the expert and the learner was evaluated. Time spent was the used characteristic. A single-factor ANOVA was used with a significance level of 0.05. We set the null hypothesis H_0 that the averages of time spent by the experts and

**Figure 15.** Time (min) to retrieve ultrasound images of reference.

learners were equal; $H_0: u_1 = u_2$ and H_1 : the averages were different. The time spent to get an US image of reference by the expert was around 5.59 min, while the mean time spent by the learner was 14.33 min as shown in Table 3. The difference between experts and learners was significant ($F = 1.99E+ 03$, $dll = 1$, $P = 1.14E-75$). We noticed that P was much less than 0.05. Regarding the test results, we rejected the null hypothesis, which proved that the simulator differentiated between the expert and the learner.

3.4 Transfer validity

This evaluated how the use of the simulator improved the learner experience on real patient. Learners were asked to evaluate their difficulty to achieve the exam on patients assuming that it had performed (or not performed) the same exam on the virtual environment.

A scoring system of level 1 to 10 (the higher the level, the most difficult the exam) was adopted. Without the use of the virtual environment, the exam was judged difficult with a score of 9 by the learners, and no learner had performed the US exam within a time out of 30 minutes. Having performed previously the exam on the virtual environment, the exam was judged easier with a score of 6.

4. Discussion and future works

A realistic low-cost US simulator has been developed. The 2D US images were simulated from acquired US volumes. The US images deformation under probe pressure is realistically simulated. Immersion in US simulation is a critical point. Simulation must go through all the senses invoked in the real exam to guaranty good conditions for the learner. It is also important to make a simulator affordable to make large use possible. Table 4 gives a

Table 4. Performance comparison of our simulator with the existing ones.

Simulator	Immersive	Affordable	Supervise
UltraSim (Aiger and Cohen-Or 1998)	No	No	No
UltraTrainer (Stalkamp and Wapler 1997)	No	No	No
SonoSim3D (Ehrlicke 1998; Petrinc 2013)	No	No	No
Paediatric simulator (Arkhurst et al. 2001)	No	Yes	No
Echocardiography simulator (Weidenbach et al. 2004)	No	No	No
Thrombosis simulator (Aulignac et al. 2006)	Yes	No	No
SonoTrainer (Maul et al. 2004)	No	No	No
TRUS (Persoon et al. 2010)	No	No	No
Echocardiogram simulator (Sun and McKenzie 2011)	No	No	No
Schallware (Breitkreutz et al. 2009)	No	No	No
TEE (Weidenbach et al. 2007)	No	No	No
Obstetric ultrasound simulator (Liu et al. 2015)	No	Yes	No
Obstetric ultrasound simulator (Lertwiram et al. 2011)	No	No	No
Our simulator	Yes	Yes	Yes

comparison between the existing simulators and the developed one in terms of immersion (US image deformation and force feedback), technology affordance and supervised learning.

As presented in Table 4, the existing simulators did not simulate US image deformation, and only the thrombosis simulator (Aulignac et al. 2006) allowed the US image deformation under probe pressure. However, it deformed the US image in a linear manner which is not realistic because of the difference between biomechanical characteristics of human tissues. The developed virtual environment simulated the applied force when performing US exam from real acquired forces. The instrumented US probe with force sensors acquired elasticity map of the region related to the studied organ. The simulated forces were transmitted to the learner via an affordable three degrees of freedom haptic joystick. In state of the art, simulators with plastic mannequin did not offer a realistic force feedback. It is known that the elasticity of human tissues is far from the plastic models. Aulignac and colleagues (Aulignac et al. 2006) simulated force feedback based on a simplified spring-mass model of the thigh and used an expensive three degrees of freedom joystick. Besides this, the US obstetrical simulator (Liu et al. 2015) was affordable, but it did not allow US image deformation and the force feedback from plastic is not realistic. The use of an adapted joystick for learning process with the adequate characteristics for US exam simulation would help to make the simulator large use.

Simulating US images is actually not sufficient to make a good learning. The learner has to be guided until the correct US image is acquired. In state of the art, proposed simulators were not interested to that aspect. The developed virtual environment included a virtual learning agent. The pedagogic agent supervised the learner and gave him directives according to the learner actual gesture (position, orientation and force) and the US exam of reference previously acquired in the learning database. The resulted outcome was than synthesised by the synthesise agent and displayed to the expert in the flow chart. The expert evaluated the learner exam and made decisions. We noticed that only the developed simulator supervised the learner in the learning process, while in all the existing simulators, the presence of the expert is still required. For the most existing simulators, few experts evaluated simulator functionalities.

In order to evaluate the developed virtual environment usability and user experience, the validation process including face, content, construct and transfer validity was adopted. In virtual reality field, immersion, interaction and perception are the fundamentals of any virtual environment. The users were asked to give their opinion on US image quality, US image deformation, credibility of interactions, force feedback intensity, probe manipulation, perception of spatial and temporal coherence. An average score of 8.37/10 was given in face validity which is actually a good score.

The proposed virtual environment usefulness and accretion of abilities were evaluated. The learners were asked to retrieve three US images of reference with the help of the intelligent agent first and then without its help. As a result, only two learners have designated the wrong US image and one was gone over the time out. The developed virtual environment well differentiated

between the learner and the expert performance. Keeping in mind the final goal is that the use of the developed virtual environment improve the learner performance on real patient, therefore transfer validation step was performed, learners when asked to perform the US exam on patient before using the US environment have found difficulties, but when learners have first experimented in the developed virtual environment and then performed the US exam on patient, the exam became easier, this confirmed the developed simulator usefulness in real life.

However, the proposed solution is limited to static anatomical structures and it is not adapted to dynamic structures such as in foetal examination. Indeed, obstetrics US simulation concept should be completely different because of random and unpredictable movement of the foetus where an US image may not be related to a reference position of the US probe. The use of six degrees of freedom joystick will improve the immersion of the learner in the proposed US learning environment. The joystick must be affordable to maintain the affordability of the virtual environment. Moreover, our US learning environment does not allow communication and collaboration between learners when performing a simulated US exam, and a collaborative intelligent agent should be included.

Currently, we are working on the extension of this simulator to moving structures such as in obstetrics. To achieve this challenging objective, we plan to simulate foetus movements by synthesising the US images using a virtual model of the foetus. The US foetus virtual environment will include a collaborative intelligent agent in order to allow collaboration between learners.

5. Conclusion

Considering the performed validation process results, an optimal, low-cost, virtual learning environment for US examination has been developed. These results are explained by the good immersion of the learner and the offered supervised learning process to guide the learner and mimic expert guidance. We illustrated how to exploit the real acquired data stored in a learning database to design a whole virtual environment. The acquisition was made possible by instrumenting an US probe such that for each US image, the probe position and orientation in 3D space and the force applied on the probe in the same and real time were recorded.

Disclosure statement

No potential conflict of interest was reported by the authors.

References

- Aiger D, Cohen-Or D. 1998. Real-time ultrasound imaging simulation. *Real-Time Imaging*. 4(4):263–274.
- Alessandrini M, de Craene M, Bernard O, Giffard-Roisin S, Allain P, Waechter-Stehle I, Weese J, Saloux E, Delingette H, Sermesant M, et al. 2015. A pipeline for the generation of realistic 3D synthetic echocardiographic sequences: methodology and open-access database. *IEEE Trans Med Imaging*. 34(7):1436–1451.
- Arkhurst W, Pommert A, Richter E, Frederking H, Kim SI, Schubert R, Höhne KH. 2001. A virtual reality training system for pediatric sonography. In: *International congress series*. Vol. 1230. Elsevier; p. 483–487. Accessed

- at <http://www.sciencedirect.com/science/article/pii/S0531513101000619>
- Aulignac D, Laugier C, Troccaz J, Vieira S. 2006. Towards a realistic echographic simulator. *Med Image Anal.* 10(1):71–81.
- Bamber JC, Dickinson RJ. 1980. Ultrasonic B-scanning: a computer simulation. *Phys Med Biol.* 25(3):463.
- Block DJ, Michelotti MB, Sreenivas RS. 2013. Application of the Novint Falcon haptic device as an actuator in real-time control. *Paladyn J Behav Robotics.* 4(3):182–193.
- Breitkreutz R, Schellhaas S, Schmitz-Rixen T, Kessler P, Walcher F. 2009. Ultrasound simulation of peripheral nerves: development of a novel technology for training in regional anaesthesia. *Crit Ultrasound J.* 1(1):5–11.
- Carter FJ, Schijven MP, Aggarwal R, Grantcharov T, Francis NK, Hanna GB, Jakimowicz JJ. 2005. Consensus guidelines for validation of virtual reality surgical simulators. *Surg Endosc Other Interv Tech.* 19(12):1523–1532.
- Chaoui J, Dardenne G, Hamitouche C, Stindel E, Roux C. 2009. Virtual movements-based calibration method of ultrasound probe for computer assisted surgery. *Biomedical Imaging: From Nano to Macro. ISBI'09. IEEE International Symposium on* 1207–1210.
- Courtecuisse H, Jung H, Allard J, Duriez C, Lee DY, Cotin S. 2010. GPU-based real-time soft tissue deformation with cutting and haptic feedback. *Prog Biophys Mol Biol.* 103(2):159–168.
- Dardenne G, Chaoui J, Hamitouche C, Stindel E, Aliotti A, Roux C. PCT/EP08855881. 2008. Method for calibrating ultrasound probes.
- Delgorgue C, Courrges F, Bassit LA, Novales C, Rosenberger C, Smith-Guerin N, Vieyres P. 2005. A tele-operated mobile ultrasound scanner using a light-weight robot. *IEEE Trans Inf Technol Biomed.* 9(1):50–58.
- Driscoll J. 2007. Practising clinical supervision: A reflective approach for health-care professionals. Elsevier Health Sciences. UK: bailliere tindall elsevier
- Ehrlicke HH. 1998. SONOSim3D: a multimedia system for sonography simulation and education with an extensible case database. *Eur J Ultrasound.* 7(3):225–230.
- El-Sana J, Varshney A. 2000. Continuously-adaptive haptic rendering. *Virtual Environments.* Vienna: Springer; p. 135–144.
- Fuchs P, Moreau G, Guitton P. 2011. Virtual reality: concepts and technologies. Boca Raton (FL): CRC Press, Inc.
- Gao H, Choi HF, Claus P, Boonen S, Jaecques S, van Lenthe GH, van der Perre G, Lauriks W, D'hooge J. 2009. A fast convolution-based methodology to simulate 2-D/3-D cardiac ultrasound images. *IEEE Trans Ultrason Ferroelectr Freq Control.* 56(2):404–409.
- Gillies DF, Williams CB. 1987. An interactive graphic simulator for the teaching of fibroendoscopic techniques. In: *Eurographics. Eurographics Association* p. 127–138.
- Goksel O, Sapchuk K, Salcudean SE. 2011. Haptic simulator for prostate brachytherapy with simulated needle and probe interaction. *IEEE Trans Haptics.* 4(3):188–198.
- Gordon MS. 1974. Cardiology patient simulator: development of an animated manikin to teach cardiovascular disease. *Am J Cardiol.* 34(3):350–355.
- Gottschalk S, Lin MC, Manocha D. 1996. OBBTree: A hierarchical structure for rapid interference detection. In *Proceedings of the 23rd ACM annual conference on Computer graphics and interactive techniques*, 171–180.
- Henry D. 2009. Outils pour la modelisation de structure et la simulation d'examen échographiques, PhD thesis, University Joseph Fourier Grenoble France.
- Hollinger A, Wanderley MM. 2006. Evaluation of commercial force-sensing resistors. In *Proceedings of International Conference on New Interfaces for Musical Expression.*
- Jensen JA. 1996. Field: A program for simulating ultrasound systems. In: *Medical & Biological Engineering and Computing*, editor. Tampere, Finland: 10th Nordicbaltic Conference on Biomedical Imaging. Vol. 4, 351–353. supplement 1, part 1.
- Kohn S, Van Lengen RH, Reis G, Bertram M, Hagen H. 2004. Ves: virtual echocardiography system. The 4th IASTED International Conference on Visualization, Imaging, and Image Processing (VIIP-04).
- Lam CK, Sundaraj K, Sulaiman MN. 2014. Computer-based virtual reality simulator for phacoemulsification cataract surgery training. *Virtual Real.* 18(4):281–293.
- Lehmann TM, Gner C, Spitzer K. 1999. Survey: interpolation methods in medical image processing. *IEEE Trans Med Imaging.* 18(11):1049–1075.
- Lertwiram S, Tanprayoon D, Prateepmanovong C, Treratanakulwong T, Charoenwet W, Kanongchaiyos P. 2011. A design and implementation for ultrasound practice system for fetal echocardiography. In *Proceedings of the 10th International Conference on Virtual Reality Continuum and Its Applications in Industry.* 367–370. ACM.
- Levine AI, DeMaria S Jr, Schwartz AD, Sim AJ. 2013. The comprehensive textbook of healthcare simulation. Verlag, NY: Springer Science and Business Media.
- Liu L, Kutarnia J, Belady P, Pedersen P. 2015. Obstetric ultrasound simulator with task-based training and assessment. *IEEE Trans Biomed Eng.* 99(1):1.
- Mantke R, Peitz U. 2011. Surgical ultrasound: an interdisciplinary approach for surgeons, internists, and ultrasound technicians. India: Thieme.
- Martin S, Hillier N. 2009. Characterisation of the Novint Falcon haptic device for application as a robot manipulator. In *Australasian Conference on Robotics and Automation (ACRA)*, 291–292.
- Maul H, Scharf A, Baier P, Wstemann M, Gnter HH, Gebauer G, Sohn C. 2004. Ultrasound simulators: experience with the SonoTrainer and comparative review of other training systems. *Ultrasound Obstetrics Gynecology.* 24(5):581–585.
- Mazzella F, Montgomery K, Latombe JC. 2002. The forcegrid: a buffer structure for haptic interaction with virtual elastic objects. In *Robotics and Automation, 2002. Proceedings. ICRA'02. IEEE International Conference on*, 939–946.
- Ourahmoune A, Hamitouche C, Larabi S. 2014. Learning ultrasound gesture database: building and application to musculoskeletal ultrasound exams. In *Conference proceedings: Annual International Conference of the IEEE Engineering in Medicine and Biology Society. IEEE Engineering in Medicine and Biology Society. Annual Conference* 1809–1812.
- Ourahmoune A, Larabi S, Hamitouche C. 2012. A survey of echographic simulators. In: *Computational modelling of objects represented in images III: fundamentals, methods and applications.* p. 273–276. Switzerland: Springer International Publishing.
- Pan Z, Cheok AD, Yang H, Zhu J, Shi J. 2006. Virtual reality and mixed reality for virtual learning environments. *Comput Graphics.* 30(1):20–28.
- Payr S. 2003. The virtual university's faculty: an overview of educational agents. *Appl Artif Intelligence.* 17(1):119.
- Persoon MC, Schout B, Martens EJ, Tjiam IM, Tielbeek AV, Scherpbier AJ, Hendriks AJ. 2010. A simulator for teaching transrectal ultrasound procedures: how useful and realistic is it? *Simul Healthcare.* 5(5):311–314.
- Peterlik I, Nouicer M, Duriez C, Cotin S, Kheddar A. 2011. Constraint-based haptic rendering of multirate compliant mechanisms. *IEEE Trans Haptics.* 4(3):175–187.
- Peters TM. 2014. Real-time simulation of transesophageal echocardiography. *Med Meets Virtual Reality 21: NextMed/MMVR.* 21(196):436.
- Petrinec K. 2013. Patient-specific interactive ultrasound image simulation based on the deformation of soft tissue. University of California. PHD of Philosophy in Computer Science.
- Pirkowski A, Kempny A. 2013. The transesophageal echocardiography simulator based on computed tomography images. *IEEE Trans Biomed Eng.* 60(2):292–299.
- Rickel J, Johnson WL. 1999. Animated agents for procedural training in virtual reality: perception, cognition and motor control. *Appl Artif Intelligence.* 13:343382.
- Rohling R, Gee A, Berman L. 1999. A comparison of freehand three-dimensional ultrasound reconstruction techniques. *Med Image Anal.* 3(4):339–359.
- Santos CT, Osrio FS. (2004). An intelligent and adaptive virtual environment and its application in distance learning. In *Proceedings of the working conference on Advanced visual interfaces*, 362–365. ACM.
- Sclaverano S, Chevreau G, Vadcard L, Mozer P, Troccaz J. 2009. BiopSym: a simulator for enhanced learning of ultrasound-guided prostate biopsy. *Stud Health Technol Inform.* 142:301–306.
- Shin D. 2017. The role of affordance in the experience of virtual reality learning: technological and affective affordances in virtual reality. *Telematics Inform.* Elsevier: Amsterdam. 34(8): 1826–1836
- Shin D, Biocca F, Choo H. 2013. Exploring the user experience of three dimensional virtual learning environments. *Behaviour Inf Technol.* 32(2):203–214.

- Sidhu HS, Olubaniyi BO, Bhatnagar G, Shuen V, Dubbins P. 2012. Role of simulation-based education in ultrasound practice training. *J Ultrasound Med.* 31(5):785–791.
- Stalkamp J, Wapler M. 1997. UltraTrainer a training system for medical ultrasound examination. *Stud Health Technol Inform.* 50:298–301.
- Storve S, Torp H. 2017. Fast simulation of dynamic ultrasound images using the GPU, in *IEEE transactions on ultrasonics. Ferroelectr Freq Control.* 64(10):1465–1477.
- Sun B, McKenzie FD. 2011. Real-time sonography simulation for medical training. *Int J Educ Inf Technol.* 5(3):328–335.
- Vidal FP, John NW, Healey AE, Gould DA. 2008. Simulation of ultrasound guided needle puncture using patient specific data with 3D textures and volume haptics. *Comput Animat Virtual Worlds.* 19(2):111–127.
- Wang D, Zhang X, Zhang Y, Xiao J. 2013. Configuration-based optimization for six degree-of-freedom haptic rendering for fine manipulation. *IEEE Trans Haptics.* 6(2):167–180.
- Weidenbach M, Drachsler H, Wild F, Kreutter S, Razek V, Grunst G, Janousek J. 2007. EchoComTEEA simulator for transoesophageal echocardiography. *Anaesthesia.* 62(4):347–353.
- Weidenbach M, Trochim S, Kreutter S, Richter C, Berlage T, Grunst G. 2004. Intelligent training system integrated in an echocardiography simulator. *Comput Biol Med.* 34(5):407–425.
- Weller R, Zachmann G. 2009. A unified approach for physically-based simulations and haptic rendering. In *Proceedings of the 2009 ACM SIGGRAPH Symposium on Video Games*, 151–159. ACM.
- Williams CJ, Edie JC, Mulloy B, Flinton DM, Harrison G. 2013. Transvaginal ultrasound simulation and its effect on trainee confidence levels: a replacement for initial clinical training? *Ultrasound.* 21(2):50–56.
- Xu D, Wang H. 2006. Intelligent agent supported personalization for virtual learning environments. *Decis Support Syst.* 42(2):825–843.
- Yipeng H, Eli G, Li-Lin L, Weidi X, Barratt C, Vercauteren T, Alison Noble J. 2017. Freehand ultrasound image simulation with spatially-conditioned generative adversarial networks. *CMMI/RAMBO/SWITCHMICCAI*. editor. *Molecular imaging, reconstruction and analysis of moving body organs, and stroke imaging and treatment, RAMBO 2017, CMMI 2017, SWITCH. Lecture Notes in Computer Science Vol. 10555, Quebec City, QC, Canada: Springer:Cham.*
- Zhuang Y, Canny J. 2000. Haptic interaction with global deformations. in *robotics and automation, 2000. Proceedings. ICRA'00. IEEE International Conference on (3)*, 2428–2433.
- Zilles CB, Salisbury JK. 1995. A constraint-based god-object method for haptic display. In *Intelligent Robots and Systems 95.'Human Robot Interaction and Cooperative Robots', Proceedings. 1995 IEEE/RSJ International Conference on (3)*, 146–151.